



CHORUS

This is the accepted manuscript made available via CHORUS. The article has been published as:

Near-complete violation of detailed balance in thermal radiation

Linxiao Zhu and Shanhui Fan

Phys. Rev. B **90**, 220301 — Published 1 December 2014

DOI: [10.1103/PhysRevB.90.220301](https://doi.org/10.1103/PhysRevB.90.220301)

Near-complete violation of detailed balance in thermal radiation

Linxiao Zhu

Department of Applied Physics, Stanford University, Stanford, California 94305, USA

Shanhui Fan*

*Department of Electrical Engineering, Ginzton Laboratory,
Stanford University, Stanford, California 94305, USA*

Abstract

We introduce general principles for achieving maximal violation of detailed balance in thermal radiation. We validate these principles by direct numerical calculations, based on fluctuational electrodynamics, on thermal emitters constructed from magneto-optical photonic crystals. Such a capability to maximally violate the detailed balance provides new opportunities for the design of thermal absorber and emitter.

For thermal radiation, the principle of detailed balance leads to the general form of the Kirchhoff's law [1–4], which states that

$$e(\omega, \theta, \phi) = \alpha(\omega, \theta, \phi) \quad (1)$$

where e is the directional spectral emissivity, α is the directional spectral absorptivity, ω is the frequency, and θ and ϕ specify a direction. Seeking to violate detailed balance is fundamentally important, because the principle of detailed balance implies the existence of an intrinsic loss mechanism that limits the efficiency of many energy conversion processes. For example, a solar absorber absorbs light from the sun. The detailed balance then dictates that the solar absorber must therefore radiate back to the sun. Such a radiation back to the sun is an intrinsic loss mechanism that can only be eliminated by maximal violation of detailed balance. The ability to significantly violate detailed balance therefore points to a previously unexplored pathway for fundamental improvement of a wide variety of energy conversion processes, including solar energy harvesting and thermal radiation energy conversion.

Microscopically, Eq. 1 can be proven using the fluctuation-dissipation theorem, but only for emitters consisting of materials satisfying Lorentz reciprocity [5, 6]. It has been noted theoretically that non-reciprocal materials, such as magneto-optical materials, may not obey detailed balance [7] and hence may not satisfy Eq. 1, without violating the second law of thermodynamics [8]. However, there has not been any direct experimental measurement or theoretical design of actual physical structures that violate detailed balance.

In recent years, significant efforts have been devoted to the use of engineered photonic structures, including photonic crystals [9–26], optical antennas [27–29] and metamaterials [30–32], for the control of thermal radiation properties. Photonic structures can exhibit thermal radiation properties that are significantly different from naturally occurring materials. Notable examples include the creation of thermal emitters with narrow spectrum [12, 15, 25] or enhanced coherence [11, 17]. All previous works on the thermal radiation properties of photonic structures, however, consider only reciprocal materials. In this Letter, using the formalism of fluctuational electrodynamics [33–37], we present a direct numerical calculation of thermal emission from non-reciprocal photonic structures, and introduce the theoretical conditions for such structures to maximally violate detailed balance, i.e. to achieve a unity difference between directional spectral emissivity and absorptivity.

Non-reciprocal photonic structures represent an important emerging direction for the control of thermal radiation. From a fundamental point of view, significant numbers of theoretical approaches for the calculations of far-field thermal radiation use the Kirchhoff's law of Eq. 1 by computing the absorption properties [15–19, 21, 22, 24]. Such an approach is no longer applicable for non-reciprocal thermal emitters, and direct calculations using the formalism of fluctuational electrodynamics become essential. From a practical point of view, creating non-reciprocal thermal emitters can have important implications for the enhancement of the efficiency for solar cells [38, 39] and thermophotovoltaic systems [40].

We start by reviewing the general thermodynamic constraints on non-reciprocal thermal emitters. Consider an emitter undergoes radiative exchange through two radiation channels, A and B , with two separate blackbodies also labelled A and B , respectively. Part of the emission from either blackbody A or blackbody B towards the emitter is absorbed, as described by absorptivities α_A and α_B , respectively. The emitter also emits towards the blackbodies as described by emissivities e_A and e_B , respectively. We consider the equilibrium situation where the emitter, and the blackbodies, are at the same temperature T . The second law of thermodynamics then requires that there is no net energy flow in or out of the emitter, independent of whether the emitter is reciprocal or not. In the reciprocal case (Fig. 1a), $\alpha_{A,B} = e_{A,B}$, and as a result the second law of thermodynamics is satisfied. In the non-reciprocal case (Fig. 1b), consider the emission from blackbody A , through channel A , we assume that the part of the emission that is not absorbed by the emitter is reflected through channel B to blackbody B , with a reflectivity $r_{A \rightarrow B}$. As a result, we have

$$\alpha_A + r_{A \rightarrow B} = 1. \quad (2)$$

On the other hand, blackbody A receives emission both from the emitter and the part of emission from blackbody B that is not absorbed by the emitter, i.e.

$$e_A + r_{B \rightarrow A} = 1. \quad (3)$$

Combining Eqs. 2 and 3 and similarly consider the energy balance of the blackbody B , we have

$$e_A - \alpha_A = r_{A \rightarrow B} - r_{B \rightarrow A} = \alpha_B - e_B \quad (4)$$

For non-reciprocal systems, $r_{A \rightarrow B} \neq r_{B \rightarrow A}$ [41–43]. As a result, $e_{A,B} \neq \alpha_{A,B}$, and the detailed balance is violated. On the other hand, from Eq. 4 there is no net energy flow in and out

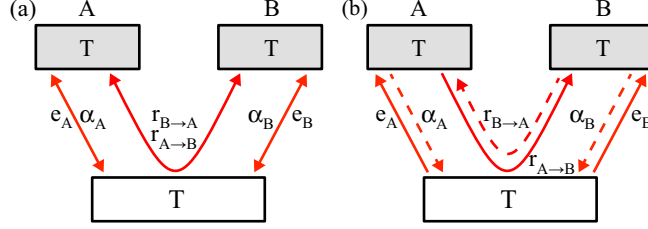


FIG. 1. (Color online). Energy flow diagrams in the cases of (a) a reciprocal emitter, and (b) a non-reciprocal emitter. The emitter undergoes radiative exchange with two separate blackbodies labelled A and B , respectively. The emitter and the blackbodies are at the same temperature T .

of the emitter as well as bodies A and B , as required by the second law. Thus, for the non-reciprocal structure considered here the second law in fact dictates the violation of detailed balance. The argument here is equivalent to Ref. [7] which uses bidirectional reflectance distribution functions, but simplified and generalized so that the argument can be directly applied to the physical system that we will consider in this Letter that has only specular reflection.

As a main contribution of this Letter, we next introduce the general conditions in order to achieve *maximum* violation of detailed balance in a physical structure. As the emitter, we consider a photonic crystal emitter structure that is periodic in x -direction, emitting to free space on top of the structure, with a mirror at the back side (Fig. 2). For simplicity we consider only a two-dimensional case where both the fields and the structure are assumed uniform along the z -direction. The principle described here however is generalizable to three dimensions. For such a structure, its electromagnetic properties are characterized by a photonic band structure $\omega(k_x)$, where ω is the frequency, and k_x is the parallel wave vector.

Corresponding to the scenario as described in Fig. 1, we study the directional spectral emissivity and absorptivity $e(\omega, \pm\theta)$ and $\alpha(\omega, \pm\theta)$, respectively, where $\pm\theta$ are the angles of incidence for the two channels. Consider light incident with an angle of incidence θ , having a parallel wavevector $k_x = \omega/c \sin\theta$. With a proper choice of periodicity that is sufficiently small, by momentum conservation, light can only be reflected into the $-\theta$ channel (Fig. 2). Moreover, if the ω and k_x of the incident light satisfy the photonic band structure $\omega(k_x)$ of the emitter, a mode inside the emitter will be resonantly excited, as a result there will typically be strong absorption, with part of the resonant excitation contributing to the reflected wave in the $-\theta$ channel. Similarly, the reflection and absorption properties for light incident with

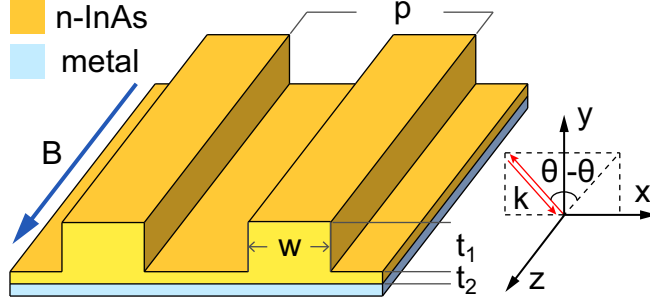


FIG. 2. (Color online). A schematic of a photonic crystal structure for maximal violation of detailed balance. The structure consists of an n-InAs grating structure atop a uniform metal layer. The structure is periodic in x -direction, and has the following geometry parameters: $p = 7.24 \mu\text{m}$, $w = 3.2 \mu\text{m}$, $t_1 = 1.981 \mu\text{m}$ and $t_2 = 0.485 \mu\text{m}$. External magnetic field is applied in z -direction. TM polarization with electric field in x - y plane is considered.

an angle of incidence of $-\theta$ will be controlled by the photonic band structure at $\omega(-k_x)$.

For an emitter constructed from a reciprocal material, its photonic band structure is symmetric in the k_x -space [44], i.e. $\omega(k_x) = \omega(-k_x)$. The resonance frequencies for lights incident with an incidence angle of either θ or $-\theta$ are the same, and $r_{\theta \rightarrow -\theta} = r_{-\theta \rightarrow \theta}$. As a result, from Eq. 4 we have $e(\omega, \pm\theta) = \alpha(\omega, \pm\theta)$, and thus detailed balance is satisfied. On the other hand, with the breaking of reciprocity, for example by the use of magneto-optical material, one can achieve an asymmetry of the photonic band structure in k_x -space [41, 45–48], i.e. $\omega(k_x) \neq \omega(-k_x)$. In such a case, the resonance conditions for the two channels are no longer the same, hence $r_{\theta \rightarrow -\theta} \neq r_{-\theta \rightarrow \theta}$, and as a result detailed balance can be violated.

In order to achieve maximum violation of detailed balance, from Eq. 4, one needs to have $r_{\theta \rightarrow -\theta} \approx 1$, and $r_{-\theta \rightarrow \theta} \approx 0$. Using coupled mode theory (CMT) [49], when the frequency of the incident light is near-resonant, one can show that

$$r(\omega)_{\theta \rightarrow -\theta} = \frac{[\omega - \omega(k_x)]^2 + (\gamma_i - \gamma_e)^2}{[\omega - \omega(k_x)]^2 + (\gamma_i + \gamma_e)^2} \quad (5)$$

and

$$r(\omega)_{-\theta \rightarrow \theta} = \frac{[\omega - \omega(-k_x)]^2 + (\gamma_i - \gamma_e)^2}{[\omega - \omega(-k_x)]^2 + (\gamma_i + \gamma_e)^2}, \quad (6)$$

where for simplicity we have assumed that the two resonances at $\omega(k_x)$ and $\omega(-k_x)$ have the same intrinsic material loss rate γ_i , and external leakage rate γ_e . Therefore, to achieve maximum violation of detailed balance, the structure needs to provide critical coupling for

light incident with an angle of θ , i.e.

$$\gamma_i = \gamma_e, \quad (7)$$

and also needs to be sufficiently off resonance for light incident with an angle of $-\theta$, i.e.

$$|\omega(k_x) - \omega(-k_x)| \gg \gamma_{i,e}. \quad (8)$$

We provide a brief comment on some of the assumptions for Eqs. 5 and 6. The coupled mode theory is valid for resonance systems having a relatively high quality factor [49] and therefore applies to our system. Also, when compared with the underlying reciprocal structure, the introduction of non-reciprocal effects typically shifts the resonance frequency by a substantial amount, without significantly influencing the intrinsic material loss rate and external leakage rate of the resonance.

We implement the general consideration above with a photonic crystal structure as shown in Fig. 2. The photonic crystal structure consists of an n-InAs grating structure with $7.24 \mu\text{m}$ periodicity, on top of a uniform metal layer acting as a mirror. For most of the calculations in the paper, we assume the mirror to be a perfect electric conductor (PEC). The effect of using a lossy aluminum mirror will be discussed towards the end of the paper. We consider the TM polarization with electric fields in the x - y plane. To break reciprocity, we use a Voigt geometry, where an external magnetic field is applied along the translation-invariant z -direction. The relative permittivity tensor of n-InAs in the presence of the B field is [50–52]:

$$\bar{\epsilon} = \begin{bmatrix} \epsilon_\infty - \frac{\omega_p^2(\omega+i\Gamma)}{\omega[(\omega+i\Gamma)^2-\omega_c^2]} & \frac{i\omega_p^2\omega_c}{\omega[(\omega+i\Gamma)^2-\omega_c^2]} & 0 \\ -\frac{i\omega_p^2\omega_c}{\omega[(\omega+i\Gamma)^2-\omega_c^2]} & \epsilon_\infty - \frac{\omega_p^2(\omega+i\Gamma)}{\omega[(\omega+i\Gamma)^2-\omega_c^2]} & 0 \\ 0 & 0 & \epsilon_\infty - \frac{\omega_p^2}{\omega(\omega+i\Gamma)} \end{bmatrix},$$

where $\epsilon_\infty = 12.37$ [53] is the high-frequency permittivity, Γ is the relaxation rate, $\omega_p = \sqrt{n_e e^2 / (m^* \epsilon_0)}$ is the plasma frequency, and $\omega_c = eB/m^*$ is the cyclotron frequency. Here n_e is the electron carrier density, m^* is effective electron mass, and B is the external magnetic field. We assume a doping concentration $n_e = 7.8 \times 10^{17} \text{ cm}^{-3}$. For the given doping level, the effective electron mass is $m^* = 0.033 m_e$ [53] (m_e is electron mass), and relaxation rate Γ is calculated from $A = 4\pi/\lambda \cdot \text{Im} \left[\sqrt{\epsilon_\infty - \frac{\omega_p^2}{\omega(\omega+i\Gamma)}} \right]$, where experimental absorbance $A = 0.0382 \times \lambda^3$ (with λ in μm , and A in cm^{-1}) is extracted from Ref. 53. We consider experimentally-achievable external magnetic field $B = 3 \text{ T}$. As our structure operates at

$T \geq 300 K$, where thermal energy is larger than Landau splitting energy $\hbar\omega_c$, Landau quantization is ignored.

The band structure of the photonic crystal can be understood by first considering a uniform slab of n-InAs with a thickness of $1.361 \mu m$, atop PEC mirror. This uniform slab contains the same amount of n-InAs per unit area as the structure in Fig. 2. Its dispersion relation $\omega(k_x)$ can be calculated from:

$$\tan(k_y t) = \frac{\epsilon_{\perp} k_y \alpha_y}{\epsilon_{\perp} (\omega/c)^2 - k_x^2 - \eta k_x \alpha_y} \quad (9)$$

where $\epsilon_{\perp} = \text{Re}(\epsilon_{xx}) = \text{Re}(\epsilon_{yy})$, gyration $\eta = \text{Im}(\epsilon_{xy}) = -\text{Im}(\epsilon_{yx})$, t is the thickness of the uniform slab, $k_y = \sqrt{(\omega/c)^2 (\epsilon_{\perp} - \eta^2/\epsilon_{\perp}) - k_x^2}$ is y -component wave vector of the guided mode inside the uniform slab, and $\alpha_y = \sqrt{k_x^2 - (\omega/c)^2}$ describes the exponential decay of the fields in vacuum. When $\eta \neq 0$, as will occur when the magnetic field is applied, we have $\omega(k_x) \neq \omega(-k_x)$.

To determine the dispersion relation of the photonic crystal, we compute the directional spectral absorptivity as shown in Fig. 3. We calculate absorptivity by a Fourier modal method adapted for non-reciprocal structures [54]. The location of the absorption peak in the ω - k_x space, which corresponds to the band structure of the photonic crystal, compares quite well with the folded band structure of the uniform slab. The effect of periodicity results in part of the band structure being folded above the light line, creating guided resonances which then manifest as absorption resonances. In Fig. 3, we observe $\omega(k_x) \neq \omega(-k_x)$ in the band structure of the photonic crystal.

In connection of the theory as shown earlier, we show the reflection spectra $r_{\theta \rightarrow -\theta}$, and $r_{-\theta \rightarrow \theta}$ in Fig. 4. In our system, the periodicity is chosen to be small enough such that only specular reflection occurs. For reciprocal system, these spectra should be the same. In the presence of B , we see a difference between $r_{\theta \rightarrow -\theta}$ and $r_{-\theta \rightarrow \theta}$. The reflection spectra agree very well with coupled mode theory fitting using Eqs. 5 and 6, as shown in Fig. 4, with the parameters of the theoretical fit included in the caption of Fig. 4. The resonances are close to the critical coupling condition, as can be seen either by noting that peak absorption approaches 100%, or by examining the relevant internal absorption and external leakage rates in Fig. 4. The resonance frequency separation $|\omega(k_x) - \omega(-k_x)|$ is much larger than the decay rates, and satisfies the requirement of Eq. 8.

The calculation above, on the absorption properties of the photonic crystal, shows that

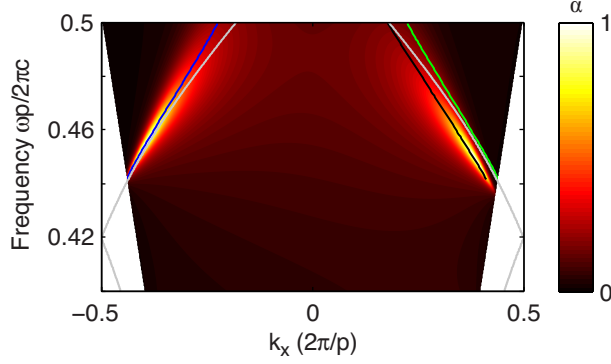


FIG. 3. (Color online). Absorptivity for different parallel wave vectors and frequencies, for the structure in Fig. 2 with PEC as mirror, at $B = 3 T$. The black and blue solid curves denote the peaks of absorptivities at positive and negative parallel wave vectors, respectively. The green solid curve is the mirror reflection of the blue solid curve. The grey solid curves denote the folded band structure for a $1.361 \mu m$ -thick uniform n-InAs atop PEC mirror without external B field.

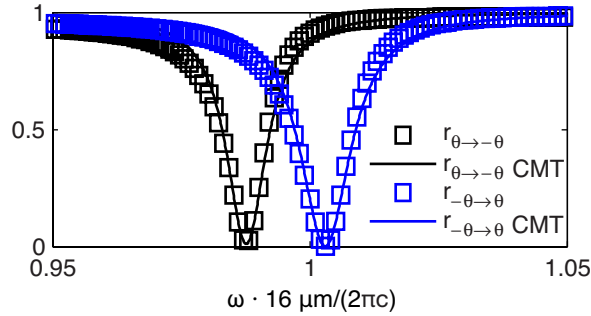


FIG. 4. (Color online). Reflectivity spectra of $r_{\theta \rightarrow -\theta}$ and $r_{-\theta \rightarrow \theta}$, for the structure in Fig. 2 with PEC mirror, at $B = 3 T$ and $\theta = 61.28^\circ$. The parameters for the coupled mode theory (CMT) fitting using Eqs. 5 and 6 are: $\omega(k_x) = 456.6 \times 10^{11} \text{ rad/s}$, $\omega(-k_x) = 463.7 \times 10^{11} \text{ rad/s}$, $\gamma_{i,k_x} = 1.22 \times 10^{11} \text{ rad/s}$, $\gamma_{e,k_x} = 9.78 \times 10^{10} \text{ rad/s}$, $\gamma_{i,-k_x} = 1.33 \times 10^{11} \text{ rad/s}$ and $\gamma_{e,-k_x} = 1.42 \times 10^{11} \text{ rad/s}$.

such a photonic crystal satisfies all the theoretical conditions for maximum violation of detailed balance. As a direct check of the theoretical concept, we now proceed to compute the directional spectral emissivity and compare that with the corresponding directional spectral absorptivity. Obviously, since our goal is to demonstrate violation of detailed balance, we cannot use absorptivity calculation to infer about emissivity, as was commonly done in the literature on thermal radiation calculation [15–19, 21, 22, 24]. Instead, to compute

emissivity, we provide a direct calculation based on fluctuational electrodynamics. In this approach, the thermal emission is generated by fluctuating random current $j(\mathbf{r}, t)$ inside the material. The magnitude of the fluctuation is related to the imaginary part of the dielectric tensor:

$$\langle j_k(\mathbf{r}, \omega) j_l^*(\mathbf{r}', \omega') \rangle = 4\pi\omega\Theta(\omega, T)\delta(\mathbf{r} - \mathbf{r}')\delta(\omega - \omega') \\ [\epsilon_{kl}(\mathbf{r}, \omega) - \epsilon_{lk}^*(\mathbf{r}, \omega)] / (2i) \quad (10)$$

where $\Theta(\omega, T) = \hbar\omega / (\exp(\hbar\omega/k_B T) - 1)$. This form of the fluctuation-dissipation theorem is appropriate for magneto-optical materials [37]. We assume the structure is in local thermal equilibrium with a uniform temperature T . To compute the resulting energy flux from such sources, we use a Fourier modal method, where the fluctuating random current $j(\mathbf{r}, t)$, the dielectric constant profile in each patterned layer, and the electromagnetic fields, are all expanded in Fourier space. We use a numerically stable scattering matrix formalism [54] to relate Fourier modal amplitudes between layers. The magnitude of the fluctuation is determined from Eq. 10.

In Fig. 5a and b, we show the emissivity spectra, for the structure atop PEC mirror (Fig. 2), at $\theta = 61.28^\circ$, and compared to the absorptivity spectra at the same angle. Figure 5a shows the calculation result when $B = 0$. The absorptivity and emissivity spectra perfectly overlap, and detailed balance is satisfied in this case as expected. We emphasize that our computation method itself does not use reciprocity. Thus the agreement of two separate calculations on absorptivity and emissivity provides a direct check of our numerical approach. With $B = 3 T$ (Fig. 5b), the absorptivity and emissivity no longer overlap, indicating the violation of detailed balance. The contrast in directional spectral absorptivity and emissivity can be as large as 12.7 dB at the wavelength of $15.92 \mu\text{m}$. Thus, our structure indeed provides near maximum violation of detailed balance. The results here provide a numerical validation of the theoretical condition.

Figure 5c shows the calculation results for the absorptivity and emissivity, when we replace the PEC mirror with a more realistic aluminum mirror. The effect of near-maximum violation of detailed balance persists. The contrast ratio between the directional spectral emissivity and absorptivity is as large as 10.2 dB at the wavelength of $15.96 \mu\text{m}$, with $\theta = 61.28^\circ$.

The capability to achieve significant violation of detailed balance may provide new op-

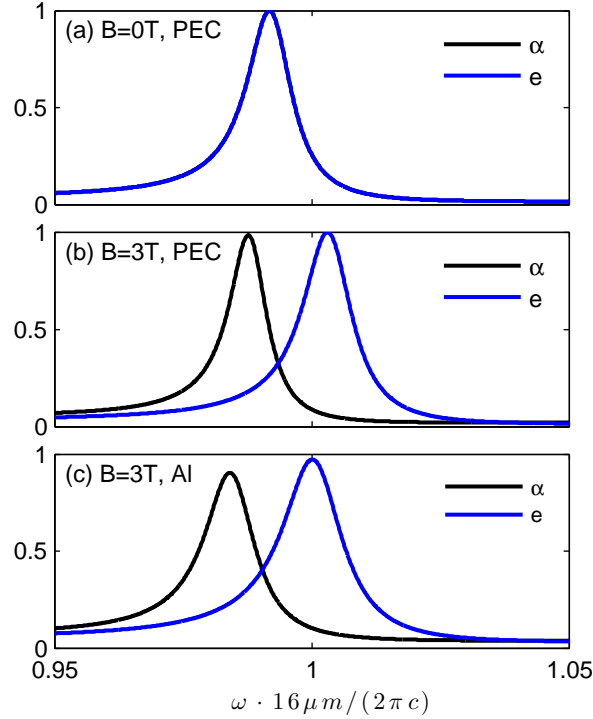


FIG. 5. (Color online). Absorptivity (α) and emissivity (e) spectra, for the structure atop PEC mirror (Fig. 2), at $\theta = 61.28^\circ$, and (a) $B = 0 T$ or (b) $B = 3 T$. (c) Absorptivity and emissivity spectra, for the structure atop aluminum (Al) mirror (Fig. 2), at $\theta = 61.28^\circ$ and $B = 3 T$.

opportunities for the design of thermal absorber and emitter. By violating detailed balance, the thermal radiation from the absorber needs not be sent to the source, but instead can be reused to boost the energy conversion efficiency [38, 39]. Our design for an thermal emitter that maximally violates detailed balance therefore points to the new opportunities to exploit non-reciprocal photonics to enhance the efficiency of renewable energy systems.

This work was supported by the DOE Light-Material Interactions in Energy Conversion Energy Frontier Research Center under grant DE-SC0001293. S. Fan acknowledges discussions with E. Yablonovitch.

* shanhui@stanford.edu

[1] G. Kirchhoff, *Annalen der Physik* **185**, 275 (1860).

[2] M. Planck, *The Theory of Heat Radiation* (P. Blakiston's Son & Co., 1914).

- [3] R. Siegel and J. Howell, *Thermal Radiation Heat Transfer, 4th Ed.* (Taylor & Francis, 2001) p. 49.
- [4] T. Bergman, A. Lavine, F. Incropera, and D. DeWitt, *Fundamentals of Heat and Mass Transfer, 7th Ed.* (Wiley, 2011) p. 811.
- [5] M. Krüger, G. Bimonte, T. Emig, and M. Kardar, Phys. Rev. B **86**, 115423 (2012).
- [6] S. E. Han, Phys. Rev. B **80**, 155108 (2009).
- [7] W. C. Snyder, Z. Wan, and X. Li, Appl. Opt. **37**, 3464 (1998).
- [8] L. Rayleigh, Nature **64**, 577 (1901).
- [9] S. Y. Lin, J. G. Fleming, E. Chow, J. Bur, K. K. Choi, and A. Goldberg, Phys. Rev. B **62**, R2243 (2000).
- [10] S. Maruyama, T. Kashiwa, H. Yugami, and M. Esashi, Appl. Phys. Lett. **79**, 1393 (2001).
- [11] J.-J. Greffet, R. Carminati, K. Joulain, J.-P. Mulet, S. Mainguy, and Y. Chen, Nature **416**, 61 (2002).
- [12] S. Y. Lin, J. Moreno, and J. G. Fleming, Appl. Phys. Lett. **83**, 380 (2003).
- [13] A. Narayanaswamy and G. Chen, Phys. Rev. B **70**, 125101 (2004).
- [14] C. Luo, A. Narayanaswamy, G. Chen, and J. D. Joannopoulos, Phys. Rev. Lett. **93**, 213905 (2004).
- [15] I. Celanovic, D. Perreault, and J. Kassakian, Phys. Rev. B **72**, 075127 (2005).
- [16] M. Florescu, H. Lee, A. J. Stimpson, and J. Dowling, Phys. Rev. A **72**, 033821 (2005).
- [17] M. Laroche, R. Carminati, and J.-J. Greffet, Phys. Rev. Lett. **96**, 123903 (2006).
- [18] D. L. C. Chan, M. Soljačić, and J. D. Joannopoulos, Phys. Rev. E **74**, 016609 (2006).
- [19] D. L. C. Chan, M. Soljačić, and J. D. Joannopoulos, Opt. Express **14**, 8785 (2006).
- [20] D. L. C. Chan, M. Soljačić, and J. D. Joannopoulos, Phys. Rev. E **74**, 036615 (2006).
- [21] S. E. Han, A. Stein, and D. J. Norris, Phys. Rev. Lett. **99**, 053906 (2007).
- [22] B. J. Lee and Z. M. Zhang, J. Heat Transfer **129**, 17 (2007).
- [23] M. Florescu, K. Busch, and J. P. Dowling, Phys. Rev. B **75**, 201101 (2007).
- [24] P. Bermel, M. Ghebrebrhan, W. Chan, Y. X. Yeng, M. Araghchini, R. Hamam, C. H. Marton, K. F. Jensen, M. Soljačić, J. D. Joannopoulos, S. G. Johnson, and I. Celanovic, Opt. Express **18**, A314 (2010).
- [25] M. D. Zoysa, T. Asano, K. Mochizuki, A. Oskooi, T. Inoue, and S. Noda, Nature Photon. **6**, 535 (2012).

- [26] K. A. Arpin, M. D. Losego, A. N. Cloud, H. Ning, J. Mallek, N. P. Sergeant, L. Zhu, Z. Yu, B. Kalanyan, G. N. Parsons, G. S. Girolami, J. R. Abelson, S. Fan, and P. V. Braun, *Nat. Commun.* **4**, 2630 (2013).
- [27] J. A. Schuller, T. Taubner, and M. L. Brongersma, *Nature Photon.* **3**, 658 (2009).
- [28] X. Liu, T. Tyler, T. Starr, A. F. Starr, N. M. Jokerst, and W. J. Padilla, *Phys. Rev. Lett.* **107**, 045901 (2011).
- [29] L. Zhu, S. Sandhu, C. Otey, S. Fan, M. B. Sinclair, and T. Shan Luk, *Appl. Phys. Lett.* **102**, 103104 (2013).
- [30] N. Dahan, Y. Gorodetski, K. Frischwasser, V. Kleiner, and E. Hasman, *Phys. Rev. Lett.* **105**, 136402 (2010).
- [31] S. Molesky, C. J. Dewalt, and Z. Jacob, *Opt. Express* **21**, A96 (2013).
- [32] M. A. Kats, R. Blanchard, S. Zhang, P. Genevet, C. Ko, S. Ramanathan, and F. Capasso, *Phys. Rev. X* **3**, 041004 (2013).
- [33] S. Rytov, Y. A. Kravtsov, and V. Tatarskii, *Principles of Statistical Radiophysics* (Springer-Verlag, Berlin, 1989).
- [34] H. B. Callen and T. A. Welton, *Phys. Rev.* **83**, 34 (1951).
- [35] R. Kubo, *Rep. Prog. Phys.* **29**, 255 (1966).
- [36] G. S. Agarwal, *Phys. Rev. A* **11**, 230 (1975).
- [37] L. Landau, E. Lifshitz, and L. Pitaevskii, *Course of Theoretical Physics Vol. 9, Statistical Physics Part 2* (Pergamon, 1980) Chap. VIII, Electromagnetic Fluctuations, p. 319.
- [38] M. Green, *Nano Lett.* **12**, 5985 (2012).
- [39] H. Ries, *Appl. Phys. B* **32**, 153 (1983).
- [40] A. Lenert, D. M. Bierman, Y. Nam, W. R. Chan, I. Celanović, M. Soljačić, and E. N. Wang, *Nature Nanotech.* **9**, 126 (2014).
- [41] Z. Yu, Z. Wang, and S. Fan, *Appl. Phys. Lett.* **90**, 121133 (2007).
- [42] D. E. Brown, T. Dumelow, T. J. Parker, K. Abraha, and D. R. Tilley, *Phys. Rev. B* **49**, 12266 (1994).
- [43] T. Dumelow and R. E. Camley, *Phys. Rev. B* **54**, 12232 (1996).
- [44] J. D. Joannopoulos, S. G. Johnson, J. N. Winn, and R. D. Meade, *Photonic Crystals: Molding the Flow of Light (Second Edition)* (Princeton University Press, 2011).
- [45] M. J. Steel, M. Levy, and R. M. Osgood, *IEEE Photon. Technol. Lett.* **12**, 1171 (2000).

- [46] I. Bitá and E. Thomas, *J. Opt. Soc. Am. B* **22**, 1199 (2005).
- [47] M. Vanwolleghem, X. Checoury, W. Śmigaj, B. Gralak, L. Magdenko, K. Postava, B. Dagens, P. Beauvillain, and J.-M. Lourtioz, *Phys. Rev. B* **80**, 121102 (2009).
- [48] A. B. Khanikaev, A. V. Baryshev, M. Inoue, and Y. S. Kivshar, *Appl. Phys. Lett.* **95**, 011101 (2009).
- [49] H. Haus, *Waves and Fields in Optoelectronics* (Prentice Hall, 1984).
- [50] K. Seeger, *Semiconductor Physics: An Introduction* (U.S. Government Printing Office, 2004).
- [51] V. I. Pipa, A. I. Liptuga, and V. Morozhenko, *J. Opt.* **15**, 075104 (2013).
- [52] S. Law, D. C. Adams, A. M. Taylor, and D. Wasserman, *Opt. Express* **20**, 12155 (2012).
- [53] O. Madelung, *Semiconductors: Data Handbook, 3rd Ed.* (Springer-Verlag, 2004).
- [54] D. M. Whittaker and I. S. Culshaw, *Phys. Rev. B* **60**, 2610 (1999).